Power System Technology
ISSN:1000-3673

Received: 06-05-2024 Revised: 15-06-2024 Accepted: 28-07-2024

Efficiency of Robust Observer Design in Power-Assisted Wheelchair Applications

[1]Kien Vu Ngoc, [2]Thanh Nguyen Thai
[1]Academy of Military Science and Technology
[2]Nguyen Trai specialized senior high school
Corresponding Author: Kien Vu Ngoc
Email: kvu3009@gmail.com

ABSTRACT: Unlike manual wheelchairs, power-assisted wheelchairs feature a unique design that allows users to combine their own propulsion with the assistive system. Recently, various studies have concentrated on the control systems for power-assisted wheelchairs. This paper introduces a 2 step control design utilizing a quasi Linear Parameter Varying (LPV) to tackle this complex control problem. The first step involves designing an observer for state and unknown input estimation. The next step proposes a controller to manage parameter including positive gains and input of the system. The control procedure is expressed as convex optimization problems with linear matrix inequality (LMI) constraints, efficiently solvable using standard numerical solvers. To validate the effectiveness of the solution, both simulations and real-time applications are performed. Both simulations and real-time experiment demonstrates that the proposed assistive control algorithm offers excellent maneuverability.

Keywords: Disabled person, Power-assisted wheelchairs, Robust torque control, Lyapunov function, Linear matrix inequality.

I. INTRODUCTION

According to the World Health Organization, a significant portion of the population in aging societies consists of disabled individuals and elderly people who have lost the ability to walk [1]. Manual wheelchairs are widely used to enhance accessibility and mobility for individuals with disabilities. Nevertheless, many users face challenges in propelling a manual wheelchair effectively due to physical limitations or varying road conditions [2]. This lack of efficiency in manual wheelchairs may lead to secondary injuries for his/her, such as joint degradation [3]. A common solution is the traditional electric wheelchair [4], [5], which supplies all the necessary power. However, this solution results in a complete cessation of physical activity for individuals,

Power System Technology
ISSN:1000-3673
Received: 06-05-2024 Revised: 15-06-2024 Accepted: 28-07-2024

which specialists do not recommend [6]. An intermediate option is power-assisted wheelchairs (PAWs), which offer an alternative by combining manual propulsion with assistive power. Manual and electric wheelchairs are typically adjusted to suit an individual's specific physical rehabilitation needs and pathology, often with the assistance of a physiotherapist.

Furthermore, designing the control for electric wheelchairs is generally straightforward. In contrast, designing control systems for assistance kits is significantly more challenging. Effectively, the assistance strategy must detect the user's intentions (such as desired velocity and the amount of assistance needed) and Supply real-time help that is secure, dependable, and easy to use. In summary, an effective assistance kit should be both 'wheelchair-neutral' and 'PRM-neutral', meaning it can function well with any wheelchair and adapt to the needs of any individual. None of the power-assisted wheelchairs kits currently available on the market are capable of meeting this challenge. Typically, the strategies employed are quite basic. Most power-assisted wheelchairs on the market offer power assistance via the hand rims that is roughly proportional to the measured person torque, but there is significant potential for improvement [7], [8], [9].

This work addresses the challenge of transitioning from initial results, which are based on his or her, fixed conditions,' to developing a solution that is as 'wheelchair-neutral' and 'PRM-neutral' as possible. The user acts as a controller, sensing the environment to produce control signals. The user collects data on their environment and their own fatigue level to make informed decisions. This information is used to determine the future trajectory of the power-assisted wheelchairs.

Previous research has tackled various aspects of observer design and desired generation. The main idea is to focus on estimating the frequency of the signals rather than their amplitude, as uncertainties may render amplitude estimates insufficiently accurate. This estimation is highly accurate for detecting the person's intentions. This work primarily focuses on the 03 point, which presents a class of problems in robust control that lacks a direct solution. For each step, LMI (Linear Matrix Inequality) constraint problems are derived, and a comprehensive proof of global closed-loop (CL) stability is presented.

The organization of this work is as follows: Section II covers the dynamic model. Section III outlines the conditions necessary for designing a controller under actuator saturations. Sections IV and V present the validation of the proposed control through simulations and real-time experiments, respectively. Section VI concludes the paper.

Power System Technology
ISSN:1000-3673
Received: 06-05-2024 Revised: 15-06-2024 Accepted: 28-07-2024

II. MATHEMATICAL MODEL

In this work, the power-assisted wheelchairs is represented as a 2-wheeled transporter. We assume that the dynamics of the caster may be ignored. Figure 1 provides a 2-dimensional overview of the power-assisted wheelchairs schematic, where φ_L and φ_R denote the left and right angular positions at wheels, respectively. The radius of the wheels is represented by *r*, the distance fors the two wheels is *h*, *a* is spacing between the point c_1 and the point c_0 and c_0 indicates the center of gravity of the power-assisted wheelchairs along with the person seated in it.

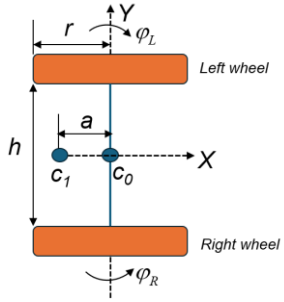

Figure 1: Model of a wheelchair

The dynamics of the 2-wheeled power-assisted wheelchairs may be presented by solving the Lagrange equation [4].

$$\begin{aligned} \delta\ddot{\varphi}_R + \gamma\ddot{\varphi}_L &= T_r - K\varphi_R \\ \delta\ddot{\varphi}_L + \gamma\ddot{\varphi}_R &= T_l - K\varphi_L \end{aligned} \rightarrow (1)$$

where the inertial parameters δ and γ are

$$\begin{aligned} \delta &= \frac{mr^2}{4} + \frac{(I_{c0} + ma^2)r^2}{h^2} I_0 \\ \gamma &= \frac{mr^2}{4} - \frac{(I_{c0} + ma^2)r^2}{h^2} \end{aligned} \rightarrow (2)$$

where, *m* represents the mass of power-assisted wheelchairs within the person, *K* denotes the viscous friction coefficient, I_{c0} denotes the inertia of the power-assisted wheelchairs with respect to the vertical axis via the point c_0 [kg/m^2], I_0 denotes the inertia of wheel [kg/m^2]. T_r and T_l are the total torques applied to the right and left wheels, respectively.

The driving surface is assumed to be flat. The total torques consist of the unknown torques T_{pr}, and T_{pl} exerted by the person, along with the motor torques T_{mr} and T_{ml} provided by the electric motors.

Power System Technology
ISSN:1000-3673
Received: 06-05-2024 Revised: 15-06-2024 Accepted: 28-07-2024

$$\begin{aligned} T_r &= T_{pr} + T_{mr} \\ T_l &= T_{pl} + T_{ml} \end{aligned} \rightarrow (3)$$

The power-assisted wheelchairs's behavior is closely linked to the user's mass and road conditions, as determined by the dynamic model (1) and the parameters (2). ω represents the speed of the center of gravity, and α denotes the yaw speed. These variables are naturally and implicitly controlled by the ones during movement and displacement.

$$\begin{bmatrix} \omega \\ \alpha \end{bmatrix} = \begin{bmatrix} \frac{r}{2} & \frac{r}{2} \\ \frac{r}{h} & -\frac{r}{h} \end{bmatrix} \begin{bmatrix} \varphi_R \\ \varphi_L \end{bmatrix} \rightarrow (4)$$

Given a sampling time $s = 50ms$, as specified by the company's device requirements, k denotes a sample. $x = [\omega \quad \alpha]^T$ the state vector, employing Euler's approximation $\dot{x} = (x_{k+1} - x_k)/s$, a discrete-time descriptor form is derived:

$$\begin{aligned} H(m)x^+ &= Ax + Bu_p + Bsat(u_m) \\ y &= Cx \end{aligned} \rightarrow (5)$$

With $y = [\varphi_R \quad \varphi_L]^T$ and $u_p = [T_{pr} \quad T_{pl}]^T$, $u_m = [T_{mr} \quad T_{ml}]^T$ the torques from the person and the motor, respectively. Both the m and K are uncertain variables and may change over time. Assuming constrained within a fixed interval.

$$m_1 \le m \le m_2; K_1 \le K \le K_2 \rightarrow (6)$$

The corresponding matrices of (5) are

$$A = \begin{bmatrix} \delta - T_e K & \delta \\ \delta & \delta - T_e K \end{bmatrix} \begin{bmatrix} 0.5r & 0.5r \\ \frac{r}{h} & -\frac{r}{h} \end{bmatrix}, B = T_e I_2$$

$$C = \begin{bmatrix} \frac{1}{r} & 0.5\frac{h}{r} \\ \frac{1}{r} & -0.5\frac{h}{r} \end{bmatrix}, E(m) = \begin{bmatrix} \delta & \gamma \\ \gamma & \delta \end{bmatrix} \begin{bmatrix} 0.5r & 0.5r \\ \frac{r}{h} & -\frac{r}{h} \end{bmatrix}$$

The mechanical model (4) is intentionally simplified. Incorporating more detailed information or modeling would require specialized knowledge, additional devices, or identification methods that are not practical for mass production of power-assisted wheelchairs kits. Although factors such as caster wheel dynamics and variations in road friction can influence the wheelchair's behavior, model (4) is expected to adequately represent the main dynamics for design for robust motion control.

Power System Technology
ISSN:1000-3673
Received: 06-05-2024 Revised: 15-06-2024 Accepted: 28-07-2024

III. ASSISTIVE SYSTEM DESIGN

The next step is to develop a robust controller that accommodates variations in mass, uncertain ground conditions, and observer biases. Additionally, the controller should be designed to perform well by smoothly tracking the reference signals ω_{des} and α_{des}, while managing saturation constraints of u_m. Designing a robust observer-based tracking controller that operates under actuator saturations does not have a straightforward solution, such as one readily available through LMI constraints.

1. Preliminaries

The tracking error of the proposed controller is:

$$\Delta_c = x_{des} - \hat{x} \rightarrow (7)$$

In which, x_{des} is the desired signal, knowing the estimated state $\hat{x} = x - \Delta_x$, where Δ_c and Δ_{int} are defined as follows:

$$\begin{aligned} \Delta_{c0} &= x_{des} + \Delta_x - x \\ \Delta_{c0}^{+} &= x_{des}^{+} + \Delta_{c0}^{+} - x^{+} \rightarrow (8) \\ \Delta_{\text{int}}^{+} &= \Delta_{\text{int}} + \Delta_c \end{aligned}$$

where the the exogenous signal together with the extended state vector are defined as follows:

$$\chi = \begin{bmatrix} u_p \\ \hat{u}_p \\ x_{des} \\ x_{des}^{+} \end{bmatrix}, \bar{\Delta} = \begin{bmatrix} \Delta_c \\ \Delta_{\text{int}} \\ \Delta_x \end{bmatrix} \rightarrow (9)$$

Thus, the dynamics of the uncertain system and the estimation error are given by:

$$\bar{H}\bar{\Delta}^{+} = \bar{A}\bar{\Delta} + \bar{B}sat(u_m) + D\chi \rightarrow (10)$$

with the matrices

$$\bar{H} = \begin{bmatrix} -H & 0 & H \\ 0 & I & 0 \\ -H + H_0 & 0 & H \end{bmatrix}, \bar{B} = \begin{bmatrix} B \\ 0 \\ 0 \end{bmatrix}, \bar{A} = \begin{bmatrix} -A & 0 & A \\ I & I & 0 \\ -A + A_0 & 0 & A - K_x C \end{bmatrix},$$

$$D = \begin{bmatrix} B & 0 & A & -H \\ 0 & 0 & 0 & 0 \\ B & -B & A - A_0 & -H + H_0 \end{bmatrix}$$

To address actuator saturations, the dead-zone function $\phi(u_m)$ is defined as follows:

$$\phi(u_m) = u_m - sat(u_m) \rightarrow (11)$$

Power System Technology
ISSN:1000-3673
Received: 06-05-2024 Revised: 15-06-2024 Accepted: 28-07-2024

Remark 1: Model (10) is presented in a descriptor form with a well-defined $\bar{H}$. By using $\bar{H}^{-1}$, one can multiply on the left in (13) to obtain an equivalent classical model. However, when formulating an LMI problem with m as an unknown parameter, it is essential to avoid increasing the number of vertices and to maintain a constant input matrix B. The descriptor form in (10) satisfies these criteria.

2. Proposed control approach

To accomplish the tracking task, the proposed control approach is expressed as follows:

$$u_m = \bar{L}\bar{M}^{-1}\bar{\Delta} + G\chi \rightarrow (12)$$

Here $\bar{L}$ and $\bar{M}$ are matrices that need to be calculated, and $G = \begin{bmatrix} 0_2 & -I_2 & G_{des} & G_{des^+} \end{bmatrix}$. Considering χ in (9), as u_p is not need to calculate directly, the first matrix of G is 0_2; The second matrix of G corresponds to the estimation of unknown $\hat{u}_p$, is install to I_2 [10]. The terms G_{des} and G_{des^+} is a feedforward controller. Note that since the tunable gains m and K are unknown that can not be included in the equation (12), as would be done in a PDC scheme [11]. Thus, the control is linear.

The observer-based CL system (10), along with the equation (12), is expressed as follows:

$$\bar{H}\bar{\Delta}^+ = (\bar{A} + \bar{B}\bar{L})\bar{\Delta} + (D + \bar{B}G)\chi - \bar{B}\phi(u_m) \rightarrow (13)$$

When combined with an anti-windup algorithm, the integral term of the tracking error is given by:

$$\Delta_{\text{int}}^+ = \Delta_{\text{int}} + \Delta_c + ES^{-T}\phi(u_m) \rightarrow (14)$$

The CL system (13) with the anti-windup algorithm (14) is expressed as follows:

$$\sum_{n=1}^{2}\varsigma_n(m)\bar{H}_n\bar{\Delta}^+ = \left(\sum_{n=1}^{2}\sum_{m=1}^{2}\varsigma_n(m)\upsilon_m(K)\bar{A}_{nm} + \bar{B}\bar{L}\bar{M}^{-1}\right)\bar{\Delta} + \left(\sum_{n=1}^{2}\sum_{m=1}^{2}\varsigma_n(m)\upsilon_m(K)D_{nm} + \bar{B}G\right)\chi + \bar{B}_a\phi(u_m) \rightarrow (15)$$

where the CL uncertain system may be expressed as a convex combination of models, with the weights influenced by the tunable gains m and K. The nonlinear functions $\varsigma_n(m)$ and $\upsilon_m(K)$ share a convex sum property, i.e. $0 \le \varsigma_n(m) \le 1$, $0 \le \upsilon_m(K) \le 1$ $\sum_{n=1}^{2}\varsigma_n(m)$ and $\sum_{n=1}^{2}\sum_{m=1}^{2}\varsigma_n(m)\upsilon_m(K) = 1$ [12]. The system matrices of (15) are $n, m \in \{0,1\}$:

Power System Technology
ISSN:1000-3673
Received: 06-05-2024 Revised: 15-06-2024 Accepted: 28-07-2024

$$\bar{H}_n = \begin{bmatrix} -H_n & 0 & H_n \\ 0 & I & 0 \\ -H_n + H_0 & 0 & H_n \end{bmatrix}, \bar{A}_{nm} = \begin{bmatrix} -A_{nm} & 0 & A_{nm} \\ I & I & 0 \\ -A_{nm} + A_0 & 0 & A_{nm} - K_x C \end{bmatrix},$$
$$\bar{B}_a = \begin{bmatrix} -B \\ ES^{-T} \\ 0 \end{bmatrix}, D_{nm} = \begin{bmatrix} B & 0 & A_{nm} & -H_n \\ 0 & 0 & 0 & 0 \\ B & -B & A_{nm} - A_0 & -H_n + H_0 \end{bmatrix}.$$

with, H_i and A_{nm} defined as:

$$H_1 = H(m_2), H_2 + H(m_1),$$
$$A_{11} = A(m_2, K_2), A_{12} = A(m_1, K_2), A_{21} = (m_2, K_1), A_{22} = A(m_1, K_1).$$

To offer the greatest flexibility and broaden the range of feasible solutions, We use a Lyapunov function that depends on parameters [13] that depends on *m* and *K*, expressed as follows:

$$V(\bar{\Delta}) = \bar{\Delta}^T \sum_{n=1}^{2} \sum_{m=1}^{2} \varsigma_n(m) \upsilon_m(\kappa) \bar{P}_{nm} \bar{\Delta} > 0 \rightarrow (16)$$

With $\bar{P}_{nm} = \bar{P}_{nm}^T \in \square^6$

Remark 2: The friction coefficient *K* may vary over time due to changes in the ground profile, and thus, K^+ will appear when constructing $V(\bar{\Delta}^+)$. However, the user's mass m remains constant for a given trajectory, making it a fixed parameter, i.e., $m^+ = m$.

Refer to Remark 2, $V(\bar{\Delta}^+)$ is given by:

$$V(\bar{\Delta}^+) = \bar{\Delta}^{+T} \sum_{n=1}^{2} \sum_{h=1}^{2} \varsigma_n(m) \upsilon_h(K^+) \bar{P}_{nh} \bar{\Delta}^+ > 0 \rightarrow (17)$$

Remark 3: Given that the output matrix *C* is a square, invertible matrix, the state vector x can be expressed as $x=C^{-1}y$. For the controller (12), the state estimation error Δ_x related to the vector $\bar{\Delta}$ is calculated as follows:

$$\Delta_x = C^{-1} y - \hat{x} \rightarrow (18)$$

IV. SIMULATION RESULTS

The advanced controller, as derived from Theorem 1, is first evaluated through simulation employing the model and controller parameters, detailed as follows: $r=3[m]$, $a=0.6[m]$, $m_0=100[kg]$, $K_0=5\ [N.m.s]$, $I_a=16[kg.m^2]$, $I_0=0.25[kg.m^2]$, $T_e=0.05s$. The variations in uncertain parameters considered for the model are: $m \in [30, 70]kg$, $3[Nms] \le K \le 7[Nms]$, encompassing most practical scenarios:

In the simulation, with $\chi \neq 0$, sinusoidal signals are utilized to depict the her/his pushing profiles. According to Remark 2, the mass remains constant for every trial, while *K* may vary over

Power System Technology
ISSN:1000-3673
Received: 06-05-2024 Revised: 15-06-2024 Accepted: 28-07-2024

time. The maximum torque of the motor is $u_{max} = 30[Nm]$ for each electric motor. Matrix $\bar{C}$ is install to: $\bar{C} = \begin{bmatrix} I_2 & 0_2 & 0_2 \\ 0_2 & 0_2 & I_2 \end{bmatrix}$.

Remark 4: During maneuvers, achieving precise turning is more crucial than maintaining speed; therefore, the yaw angle is prioritized over the center speed tracking. The matrix C is used similarly to the weighting matrix in a Linear-Quadratic Regulator design. It is install up to ensure that, in the event of actuator saturations, the equation (12) focuses first on yaw speed tracking.

Applying the design procedure from [14] with the model parameters $m_0=110kg$ and $K_0=6N.m.s$, the state observer gain K_x, K_{up} are calculated as follows:

$$K_x = \begin{bmatrix} 19.76 & -11.56 \\ -11.56 & 19.76 \end{bmatrix}, K_{up} = \begin{bmatrix} 153.71 & -82.54 \\ 162.16 & -95.91 \\ -82.54 & 153.71 \\ -95.91 & 162.16 \end{bmatrix}$$

Thus, the controller parameters determined by Theorem 1 are specified as:

$$\bar{L}\bar{M}^{-1} = \begin{bmatrix} 171.21 & 651.19 & 138.72 & 186.83 & -25.27 & -529.83 \\ 266.34 & -654.89 & 145.26 & -134.95 & -142.26 & 595.72 \end{bmatrix}$$

$$G = \begin{bmatrix} 0 & 0 & -1 & 0 & -11.33 & -235.3 & 14.24 & 258.26 \\ 0 & 0 & 0 & -1 & -164.86 & 838.01 & 171.55 & -838.41 \end{bmatrix},$$

$$ES^{-T} = \begin{bmatrix} -0.0065 & -0.0065 \\ -0.0015 & 0.0003 \end{bmatrix}, \varepsilon = 0.14 \quad and \quad \sqrt{\gamma} = 2816$$

Several simulations is conducted to validate the approach. One such simulation demonstrates the strategy's performance under uncertain parameter. In this case, the mass is instal to $m=135kg$, the viscous friction coefficient to $K=7.5Nms$, and person torques are simulated with sinusoidal input. To illustrate the algorithm's capabilities, the simulation uses trajectories corresponding to the yellow curves in Figure 5 (right) and deliberately asymmetric pushing as shown in Figure 4, with amplitudes designed to induce saturation effects. Figure 2 illustrates the torques as in blue and the estimation biases as in red caused by uncertainties in mass and friction. The observed asymmetry is primarily due to the differing frequencies of the left and right signals.

Even with the biases and asymmetry depicted in Figure 3 (right), the signal frequencies are estimated accurately, and the system performs well. On the left side of Figure 3, the motor torques necessary to follow the desired trajectories for center speed (top) and yaw speed (bottom) are presented. Saturation is indicated by the red and blue lines on the left side, Figure 3 illustrates the algorithm implemented during these moments (marked by arrows): ensuring precise tracking of the yaw speed while gradually decreasing the tracking accuracy of the center speed.

Power System Technology
ISSN:1000-3673
Received: 06-05-2024 Revised: 15-06-2024 Accepted: 28-07-2024

The simulation process was conducted extensively to address robustness issues, such as noise, uncertainties, saturations, different chair configurations, user behaviors, and pushing asymmetry, before progressing to real-time experiments.

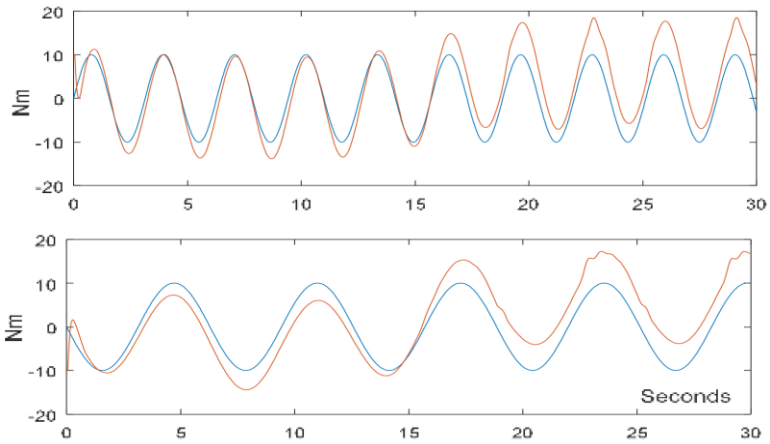

Figure 2: Emulated torques are shown in blue, while estimated person torques are depicted in red

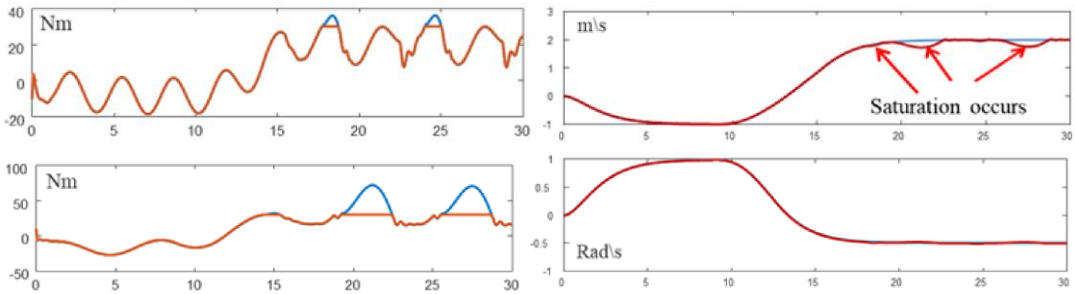

Figure 3: Motor torques with actuator saturation are shown on the left, while the desired center speed and yaw speed of the wheelchair are depicted on the right

V. EXPERIMENTAL STUDIES

Hardware-in-the-loop experimental results was carried out using a fully equipped wheelchair, with support from the company's experts. Figure 4 shows two users performing tests with the same controller and strategy. User A weighs *62kg* (resulting in a total mass of *105kg* with the wheelchair), while User B weighs *86kg* (resulting in a total mass of *135kg* with the wheelchair). Various types of terrain are used for testing, allowing for transitions between different surfaces.

Power System Technology
ISSN:1000-3673
Received: 06-05-2024 Revised: 15-06-2024 Accepted: 28-07-2024

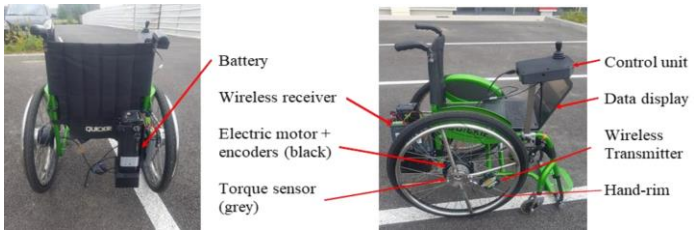

Figure 4. The components of power-assisted wheelchairs prototype

Figure 4 illustrates the power-assisted wheelchair prototype, featuring 02 brushless direct current motors powered by a battery. Each motor provides a maximum torque of approximately *42Nm*. The voltage as control signals are managed by a Texas Instruments C4000 real-time microcontroller. The system is equipped with two incremental encoders that measure angular speeds and produce pulse signals. The count of pulses within a given the sampling time is used to calculate the relative position for consecutive measurement. Additionally, two wireless torque sensors from CapInstrumentation are installed. These sensors are mounted on the prototype solely for the purpose of validating the observer.

The power-assisted wheelchair illuatrated in Figure 4 with 02 brushless direct current motors powered by a battery. Every motor gives a maximum torque of approximately *42Nm*. The inputs are managed by a Texas Instruments C4000 real-time microcontroller. The system includes 02 incremental encoders to measure speeds of wheels, outputting pulse signals. The number of pulses based on encoders is counted within a given sampling time to determine the relative position for measurements. Additionally, 02 torque devices with wireless transmission, supplied by Cap-Instrumentation, are installed. These devices are available on the prototype solely for observer validation purposes.

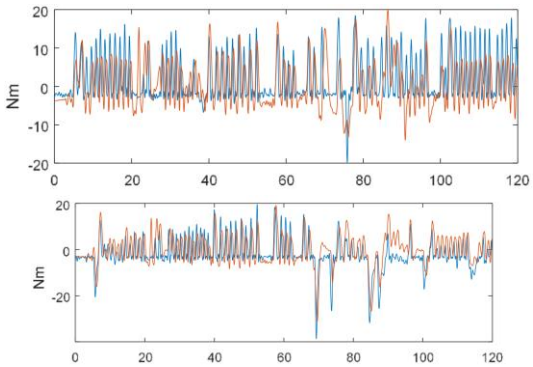

Figure 5: Human torque estimation for his/her A (top) and his/her B (bottom) on the left. Measurements are depicted in blue, while estimations are shown in red.

Power System Technology
ISSN:1000-3673
Received: 06-05-2024 Revised: 15-06-2024 Accepted: 28-07-2024

The test shown in Figure 5 involves a real-time 120-second trial conducted with both his/her across various ground profiles. The only requirement was for his/her to move straight ahead. Due to variations in ground conditions and slopes, they occasionally needed to brake one of the wheels to keep a straight trajectory.

In Figure 5, the top section shows data for his/her A and the bottom section for his/her B. The estimation signals are shown in red, and the measured torques are in blue. As anticipated, the estimated person torques do not perfectly match the measured values due to many external factors such as weather, vibration, noise. However, the estimated torques effectively capture the 02 key aspects of propulsion for both his/her: direction and pushing frequency.

VI. FUTURE DIRECTIONS AND CONCLUSIONS

The aim of this study was to develop a algorithm for the power-assisted wheelchair kits with the goal of creating a 'wheelchair-neutral' and 'PRM-neutral' kit. This algorithm consists of 03 steps: robust torque estimation to eliminate the need for torque devices and reduce costs, converting perceived intentions into control-compatible signals, and designing a robust observer-based tracking controller. 02 step Linear Matrix Inequality optimization problem has been derived using a quasi-LPV formulation alongside a descriptor representation. The first step involves designing a PI-observer, while the next step focuses on designing the controller to ensure both the stability of the CL system and the tracking performance.

The test results involved a step-by-step procedure to validate the PI observer including pushing frequency and direction, the desired generation algorithm, and the overall assistive control system.

For future work, a Deep Deterministic Policy Gradient algorithm capable of adapting to different her/his may be integrated into the current assistive control algorithm.

REFERENCES

[1]. World Health Organization, World report on disability. World Health Organization, 2011.
[2]. Cooper, R. A., Fitzgerald, S. G., Boninger, M. L., Prins, K., Rentschler, A. J., Arva, J., and O'Connor, T. J.. Evaluation of a pushrimactivated, power-assisted wheelchair. Archives of Physical Medicine and Rehabilitation, 2001, 82(5), p.702-708.
[3]. Algood, S. D., Cooper, R. A., Fitzgerald, S. G., Cooper, R., and Boninger, M. L. . Impact of a pushrim-activated power-assisted wheelchair on the metabolic demands, stroke frequency, and range of motion among subjects with tetraplegia. Archives of Physical Medicine and Rehabilitation, 2004, 85(11), p.1865-1871.

Power System Technology
ISSN:1000-3673
Received: 06-05-2024 Revised: 15-06-2024 Accepted: 28-07-2024

[4]. Tsai, M. C., and Hsueh, P. W.. Synchronized motion control for 2D joystick-based electric wheelchair driven by two wheel motors. In 2012 IEEE/ASME International Conference on Advanced Intelligent Mechatronics (AIM), 2012, p. 702-707.
[5]. Feng, G., Guerra, T.M., Busoniu, L., Nguyen, A.T. and Mohammad, S.. Robust observer-based tracking control under actuator constraints for power-assisted wheelchairs. Control Engineering Practice, 2021, 109, p.104716.
[6]. De La Cruz, C., Bastos, T. F., and Carelli, R.. Adaptive motion control law of a robotic wheelchair. Control Engineering Practice, 2011, 19(2), 113-125.
[7]. Khalili, M., Eugenio, A., Wood, A., Van der Loos, M., Mortenson, W.B. and Borisoff, J., 2023. Perceptions of power-assist devices: Interviews with manual wheelchair users. Disability and Rehabilitation: Assistive Technology, 18(5), pp.693-703.
[8]. Cornagliotto, V., Polito, M., Gastaldi, L. and Pastorelli, S.. Comprehensive control strategy design for a wheelchair power-assist device. In International Workshop IFToMM for Sustainable Development Goals 2023, p.162-170.
[9]. Tederko, P., Frasuńska, J., Bobecka Wesołowska, K., Wesołowski, K., Czech, J., Gawlak, D. and Tarnacka, B. Factors associated with employment of powered wheelchair users. Disability and Rehabilitation: Assistive Technology, 2024, p.1-8.
[10]. Chen W.H., Yang J., Guo L. and Li, S.. Disturbance-observer-based control and related methods – An overview. IEEE T. Industrial Electronics, 2015, 63 (2), p.1083-1095.
[11]. Koenig D., Mammar S. Design of proportional-integral observer for unknown input descriptor systems. IEEE T. automatic control, 2002, 47(12), p2057-2062.
[12]. Tanaka K., Wang H.O. Fuzzy control systems design and analysis: a linear matrix inequality approach. New York: John Wiley & Sons, 2001.
[13]. Guerra T.M., Vermeiren L. LMI-based relaxed non-quadratic stabilization conditions for nonlinear systems in the Takagi–Sugeno's form. Automatica 2004, 40, p.823–829.
[14]. Feng G., Guerra T.M., Busoniu L., Mohammad S. Unknown input observer in descriptor form via LMIs for power-assisted wheelchairs. 36th IEEE Chinese Control Conference (CCC), 2017, p.6299-6304.